Characterization of Below Threshold Harmonics Generated in Argon by Ultrashort Laser Pulses

Armando V. F. Zuffi
IPEN – CNEN/SP
São Paulo, Brazil
armandozuffi@gmail.com

Andreia A. Almeida
IPEN – CNEN/SP
São Paulo, Brazil
aalmeida.fis@gmail.com

Nilson D. Viera Jr.
IPEN – CNEN/SP
São Paulo, Brazil
nilsondiasvieirajr@gmail.com

Ricardo E. Samad
IPEN – CNEN/SP
São Paulo, Brazil
resamad@gmail.com

Abstract—This work reports studies on the generation of below threshold harmonics by ultrashort laser pulses in gas nozzles in vacuum. Odd harmonics of the laser, ranging from the 3rd up to the 9th, were generated in the UV and VUV regions, and the frequency conversion occurred in flowing gas. The harmonics were spectrally characterized, and the orders of the nonlinear processes were determined, showing that, for the higher order harmonics, competing processes decrease the energy coupling into the new frequencies. Also, the conversion efficiencies were estimated, showing that a few percent of the laser pulse energy are converted into the harmonics.

Keywords—nonlinear optics, harmonic generation, ultrafast optics, plasma physics, ultrashort pulses.

I. INTRODUCTION

Recently, the generation of harmonics by ultrashort laser pulses has been studied below the ionization threshold of gases [1-4]. These Below Threshold Harmonics (BTH) have an enormous potential for coherent light generation in the VUV region, being of fundamental interest for time resolved spectroscopy [5-7]. In addition, the electronic dynamics close to the ionization energy has been studied from BTH [1, 8, 9].

The BTH generation in gases presents several advantages over the generation in solids. The first one is the coherent light generation at wavelengths below 200 nm, where the solids become opaque [10]. The harmonic generation in solids below 200 nm is only possible using sophisticated techniques [11-13], while in noble gases, the absorption edge is located at their first ionization energies, which allows the generation of harmonics up to 50.4 nm in helium, as an example [14]. In addition, due to the abrupt decrease of the generation efficiency with increasing harmonic order, intensities over tens of GW/cm^2 are needed to generate the 5th and higher order harmonics. These intensities easily induce self-focusing of the beam by the Kerr effect [15], promoting damages in the solids, making the generation process unfeasible.

On the other hand, the BTH generation in gases demands intensities higher than in the solids because the density of generating centers is two orders of magnitude smaller than those of the solids [15]. Ultrashort pulses are used to generate harmonics above the 5th since they easily reach hundreds of TW/cm^2 with modest focuses. At these intensities, the pulses ionize a portion of the gas during their propagation and begin to interact with the plasma generated. This plasma can impair the efficiency of the harmonics generation. Therefore, it is required to balance the pulse intensity to efficiently generate the harmonics without wasting energy in plasma creation. An alternative is to work in vacuum, restricting the presence of the gas only to the region of the harmonics generation. In this way, ultrashort pulses interact with the gas in a nozzle a few millimeters long [16]. With this, it is expected to efficiently generate harmonics (> 1%) by the frequency conversion process in noble gases. This makes possible to carry out studies aiming at a better understanding of the phenomena involved, as well as providing a light source in the UV and VUV regions for future applications.

In this work we report the generation of BTH in argon flowing through a nozzle inside a vacuum chamber, by ultrashort pulses. Their identification and characterization are discussed, as well as competing effects that interfere on the generation.

II. EXPERIMENTAL SETUP

For the generation of BTH from the 3rd up to the 9th harmonic, pulses from a Ti:Sapphire CPA laser were used. The laser system is composed by a main oscillator (Femtolasers Rainbow) that generates 2.4 nJ, 6 fs pulses (FWHM) with, at 78 MHz, with 370 nm of bandwidth at -10 dB. This oscillator is pumped by a Coherent Verdi V6 laser. The pulses generated by this oscillator are injected into the CPA amplifier (Femtolasers Femtopower Compact Pro HR/HP). The amplification process produces pulses centered at 781 nm with 35 nm of bandwidth (FWHM), up to 650 μJ, 25 fs (FWHM), at 4 kHz repetition rate, in a laser beam with a M^2 factor of 1.5. The CPA laser system is pumped by a Q-Switched Nd:YLF laser (Photonics Industries DM30-527) that emits up to 10 mJ, 300 ns laser pulses.

The harmonics are generated inside of a 50 L, 50 cm diameter vacuum chamber, with several accesses for beam injection and instrumentation, as shown in the Fig. 1 scheme. The vacuum is achieved by a TMH 521/TMU 521 turbomolecular pump, backed by a mechanical pump, producing final pressures under 10^{-6} mbar inside the chamber. To generate the harmonics, the laser pulses are focused by a 50 cm focal length lens in a gas nozzle that is inside the vacuum chamber. The nozzle consists of a 2.3 mm internal diameter glass capillary, which is etched by ultrashort pulses in a homemade machining system to reduce its wall thickness, so it can be drilled by the same beam that generates the harmonics. This sets in the nozzle a 2.7 mm interaction length, as shown in Fig. 2, bored by the laser on 2 diametrically opposite spots. Through these holes, argon flows at a 100 mbar pressure, and the laser enters and exits the interaction region. The harmonics wavelengths can be filtered out by a glass blade that can be placed after the nozzle by vacuum compatible displacement actuators

978-1-5386-6702-6/18/$31.00 ©2018 IEEE

(Newport NSA12V6) controlled by a computer. The harmonics are separated by a VUV monochromator (McPherson 234/302). This monochromator covers the spectral range from 30 to 300 nm and has a concave 1200 g/mm holographic diffraction grating with 200 mm of focal length, f/4.5 aperture, and resolution of 1 Å. The detection is made by a photomultiplier tube (PMT) with a scintillator coated with sodium salicylate. The harmonics signal is sent to a Lock-In and stored on a computer.

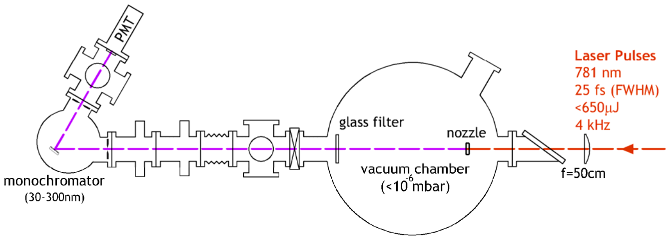

Fig. 1. Scheme of the experimental setup in which the harmonics were generated and measured.

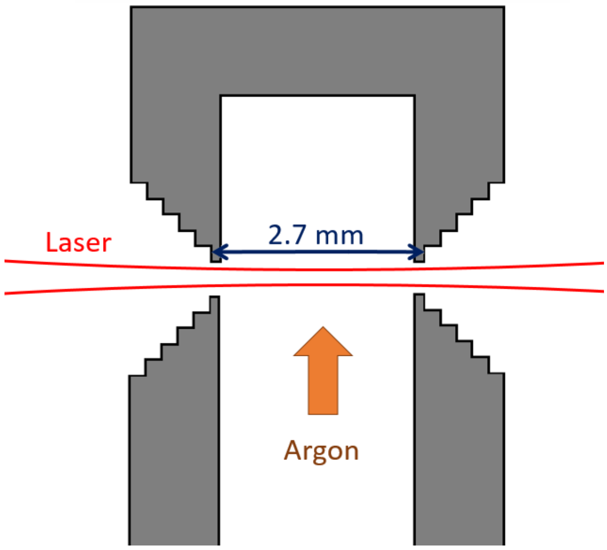

Fig. 2. Scheme of the glass nozzle. The laser beam diameter ($1/e^2$) is represented by the red lines.

Fig. 3 shows the laser spectrum measured inside the vacuum chamber before the nozzle. This spectrum was used to determine the pulses bandwidth, $\Delta\lambda_0$, and their center of mass, $\lambda_{CM,0}$, defined by:

$$\lambda_{CM} = \int \lambda\, I(\lambda)/d\lambda \,/ \int I(\lambda)/d\lambda, \qquad (1)$$

where λ is the wavelength and I is the intensity signal.

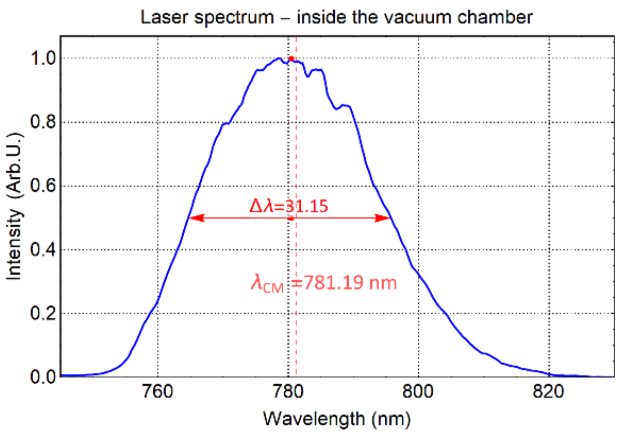

Fig. 3. Laser Spectrum after injection in the vacuum chamber.

Besides that, the transverse profiles of the laser beam are Gaussian and, at the focus, the beamwaist size is about 35 µm, as shown in Fig. 4. Therefore, the system can reach intensities higher than 10^{14} W/cm².

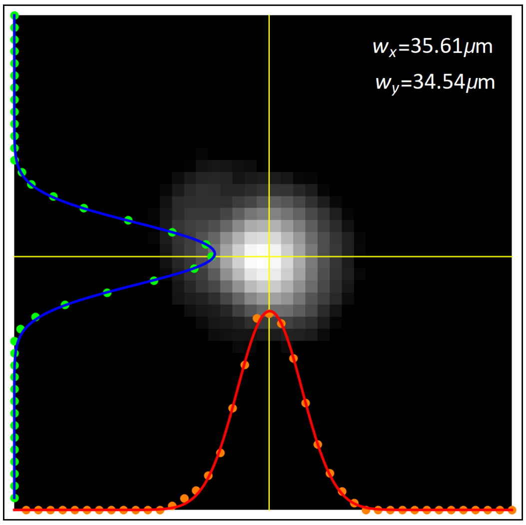

Fig. 4. Image of laser beam at the focus, showing a 35 µm beamwaist. Measurement obtained by a CCD with a pixel size of 6.7 × 6.7 µm².

III. Results

A. *Detecting the BTH in argon*

Fig. 5 shows the spectrum measured between 80 and 280 nm obtained for a laser intensity of 3.4×10^{14} W/cm² and a pressure of 100 mbar in the nozzle. This spectrum covers all harmonics generated in argon below the absorption threshold (79.0 nm), which corresponds to the argon first ionization at 15.7 eV [14]. The red vertical lines mark the theoretical positions of the spectral center of mass of the harmonics: 260.40 nm, 156.24 nm, 111.60 nm and 86.80 nm for the 3^{rd}, 5^{th}, 7^{th} and 9^{th} harmonics, respectively. They were calculated from the spectrum shown in Fig. 3.

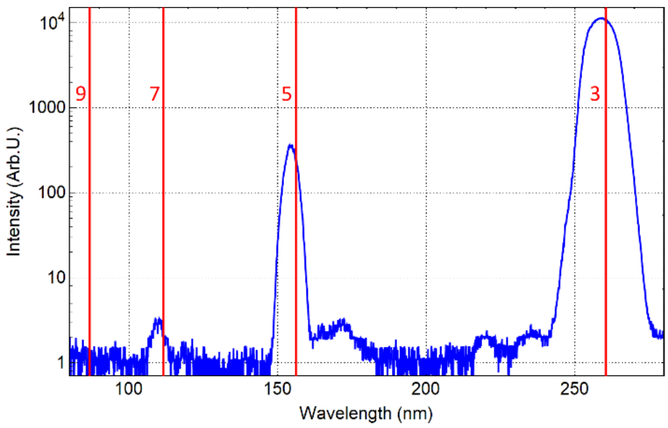

Fig. 5. Spectrum of the BTH generated in argon.

In Fig. 5, the 3rd, 5th, and 7th harmonics are clearly seen, and the generation efficiency is observed to rapidly decline with the harmonic order increase, dropping approximately two orders of magnitude from one harmonic to the next. Microscopically, this drop can be explained by the decrease of the susceptibilities of the nonlinear polarization term [15]. The 9th harmonic cannot be observed in Fig. 5 due to this efficiency decrease and the low signal-to-noise ratio in this spectrum, which spans 4 orders of magnitude.

To observe the 9th harmonic the laser pulse intensity was increased to 5.8×10^{14} W/cm², and a contrast technique with a glass slide filter was used [17]. Comparing the spectrum with and without the glass slide, the 9th harmonic is detected, as depicted in Fig. 6. This graph also shows that the detection system has a background signal coming from scatterings of the laser wavelength (orange line), which can mask the 9th harmonic signal.

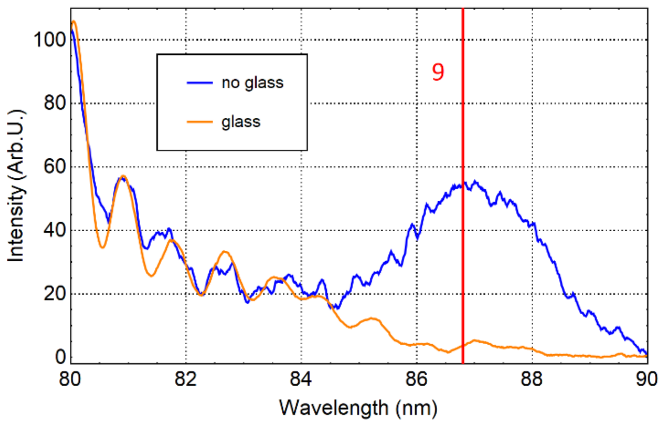

Fig. 6. 9th harmonic generated in argon.

B. *Spectral characterization of the BTH in argon*

The positions of the spectral centers of mass and the bandwidths of the harmonics generated in argon were measured from the spectra shown in Fig. 7, and the results are summarized in Table I.

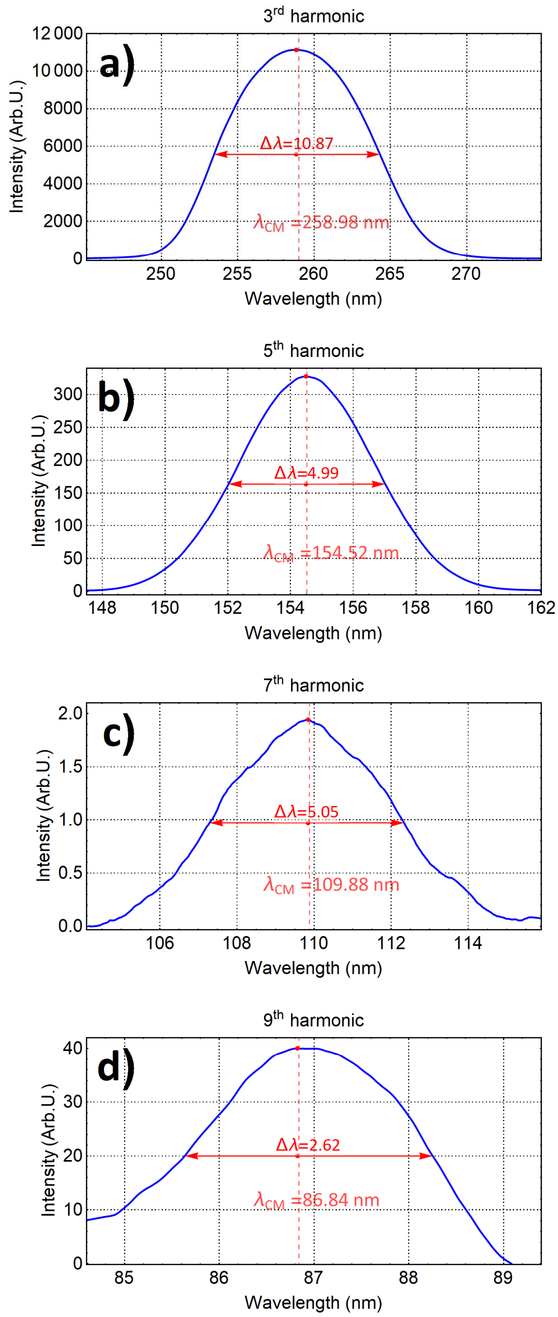

Fig. 7. Spectral characterization of a) 3rd b) 5th c) 7th and d) 9th harmonic.

Table I shows a comparison of the experimental and theoretical values of the position of the centers of mass of the spectra of the harmonics and their bandwidths. The theoretical values were calculated from the laser spectrum (Fig. 3) considering $\Delta\lambda_q=\Delta\lambda_0/q$ and $\lambda_{CM,q}=\lambda_{CM,0}/q$. The uncertainties were obtained from Gaussian fittings by the least-squares method.

TABLE I. BTH SPECTRAL CHARACTERIZATION

order	*λ_{CM} theor. (nm)*	*λ_{CM} exp. (nm)*	*Δλ theor. (nm)*	*Δλ exp. (nm)*
3rd	260.40 ± 0.02	258.98 ± 0.01	10.38 ± 0.05	10.87 ± 0.05
5th	156.24 ± 0.01	154.52 ± 0.01	6.23 ± 0.03	4.99 ± 0.01
7th	111.60 ± 0.01	109.88 ± 0.01	4.45 ± 0.02	5.05 ± 0.11
9th	86.80 ± 0.01	86.84 ± 0.01	3.46 ± 0.02	2.62 ± 0.03

The results of Table I show that the experimental and theoretical positions of the harmonics centers of mass are the same within 1%. This displacement is a consequence of the plasma induced blueshift [18, 19], and its maximum percentage displacement can be estimated by [17]:

$$\delta\omega_{max}=\sqrt{[m\ ln(2)/\pi]L\eta pN_{atm}/(c\tau_p N_{crit})} \quad (2)$$

where L = 2.7 mm is the interaction length of the nozzle, η is the average value of the ionization fraction which will be assumed to be 1% [20], p = 0.0987 atm is the nozzle pressure in atm, $N_{atm} = 2.7\times10^{20}$ $N^{-1}m^{-1}$ is the density of atoms per unit of pressure [17], c is the speed of light in vacuum, τ_p = 25 fs is the pulse duration (FWHM), N_{crit} is the critical density of free electrons in the medium [21], which is 1.8×10^{21} cm^{-3} for argon, and m is the multiphotonic absorption process order; it is assumed that ionization occurs only by a multiphotonic absorption of order 10. Such consideration is plausible since the Keldysh parameter [22] under our experimental conditions was found to be 0.8, indicating that the ionization occurs preferentially by this process instead of tunneling. With these considerations, expression (2) returns $\delta\omega_{max}$ = 0.8%, which is compatible with the displacements shown in Table I, indicating that its origin is, most probably, the plasma blueshift.

The theoretical and experimental values of the spectral centers of mass and bandwidths of the harmonics are close enough to the point that confirms that they are BTH, therefore showing that the methodology used is adequate for the generation and detection of these harmonics. The discrepancies between the theoretical and experimental values of the bandwidths should be a consequence of the competition between the nonlinear processes.

C. Analysis of the nonlinear process order

According to the microscopic properties, the intensity of the BTH increases exponentially with the laser intensity, and the exponent is equal to the order of the nonlinear process that generates the harmonic. To determine this order, the harmonic intensity signal dependence on the laser pulse intensity was measured, and this was done setting the monochromator wavelength at the position of the center of mass. These measurements were performed for laser intensities up to 1.4×10^{14} W/cm², since at higher values the plasma formation impairs the harmonic generation efficiency, saturating the signal. The results of each harmonic were fitted by:

$$I_H = Amp\ I^n, \quad (3)$$

where I_H is harmonic intensity, I is the laser pulse intensity, *Amp* is a constant of proportionality, and the exponent n provides the nonlinear process order. The results for the 3rd, 5th and 7th harmonics are shown in Fig. 8. For the 7th harmonic the data below 0.6×10^{14} W/cm² were not considered in the fitting because they deviate from the expected behavior due to the small signal and high noise-to-signal ratio measured. The order of the process for the 9th harmonic was not determined due to the difficulty of detecting its signal for the reasons already exposed.

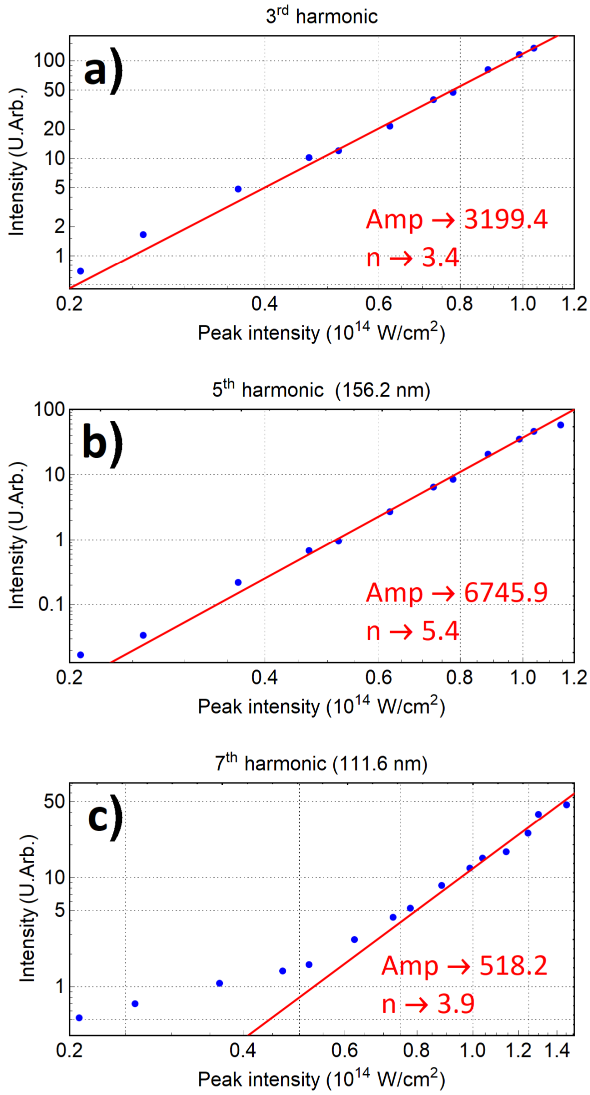

Fig. 8. Analysis of the order of the nonlinear process of the a) 3rd b) 5th and c) 7th harmonics in argon.

For the 3rd and 5th harmonics the exponent n obtained from the fitting is very close to the order of the nonlinear process, 3.4 and 5.4, respectively. However, for the 7th harmonic the exponent n=3.9 is well below 7. This can be a consequence of the noisy signal of the 7th harmonic, or a decrease of the signal due to a phase-mismatch during the generation [17]. The phase mismatch has a bigger effect on the 7th than on the other harmonics because the nozzle interaction length corresponds to 37% of the coherence length for this harmonic, decreasing its generation efficiency; for the 3rd and the 5th, the interaction length is above 80% of their coherence length, almost at the maximum generation efficiency [17]. These results are very important to confirm the generation of BTH.

D. Efficiency of energy conversion of the harmonic generation in argon

Since it is difficult to directly measure the energy contained in each harmonic pulse due to their wavelengths, an estimate of the laser pulse energy percentage that is converted into the harmonics was made.

First, the relative energy contained in each harmonic (proportional to the area of the harmonic spectrum) was determined from Fig. 5. The energy contained in the 5th harmonic is about 1% of the 3rd harmonic energy. This percentage is approximately the same for the 7th harmonic relative to the 5th. Therefore, it was assumed that the 3rd harmonic contains about 1% of the laser pulse energy. Additionally, it is known that part of the laser energy is spent on plasma generation, Kerr effect [15] and HHG [23, 24].

To estimate the portion of energy that is converted to other nonlinear effects besides the BTH, the pulse energy was measured after the nozzle, with and without gas under 100 mbar of pressure inside it. In addition, measurements were performed for different laser pulse intensities. The results are presented in Fig. 9, which shows the ratio of the pulse energies measured with gas and without gas.

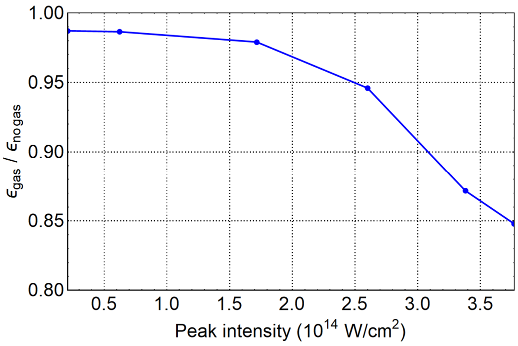

Fig. 9. Ratio of the energy of the laser pulse transmitted by the nozzle with and without gas as a function of the laser pulse intensity.

For small intensities, more than 98% of the pulse energy is transmitted through the nozzle with gas flowing. As the intensity increases, a larger fraction of the energy is converted to nonlinear phenomena. For 3.5×10^{14} W/cm² almost 15% of the laser pulse energy is converted. If 1% is converted into BTH generation, a large portion will be used in plasma formation, Kerr effect or other phenomena. Therefore, there are many nonlinear phenomena occurring simultaneously to the BTH which are responsible for a large portion of the converted energy.

IV. Conclusions

The mapping performed in this work is of fundamental importance because it presents an approach poorly explored in the literature, which is the generation of BTH in conjunction with the formation of plasma and the occurrence of other nonlinear phenomena in an experimental setup commonly used for HHG. Moreover, we performed spectral characterization and evaluated the nonlinear process order of these harmonics. Finally, we checked the percentage of laser pulse energy that converted nonlinear processes in argon, estimating the conversion efficiency.

Acknowledgment

The authors would like to acknowledge the financial support from FAPESP, CNPq and SAE, and a CAPES scholarship to one of us (Zuffi).

References

[1] Xiong, W.H., Geng, J.W., Tang, J.Y., Peng, L.Y., and Gong, Q.H., "Mechanisms of Below-Threshold Harmonic Generation in Atoms", Phys. Rev. Lett., 112(23), pp. 1-5, 2014.

[2] Hostetter, J.A., Tate, J.L., Schafer, K.J., and Gaarde, M.B., "Semiclassical approaches to below-threshold harmonics", Phys. Rev. A, 82(2), pp. 1-8, 2010.

[3] Yost, D.C., "Vacuum-ultraviolet frequency combs from below-threshold harmonics", Nat. Phys., 5(11), pp. 815-820, 2009.

[4] Lhuillier, A., Schafer, K.J., and Kulander, K.C., "Theoretical Aspects of Intense Field Harmonic-Generation", J. Phys. B-At. Mol. Opt., 24(15), pp. 3315-3341, 1991.

[5] Nabekawa, Y., "Sub-10-fs control of dissociation pathways in the hydrogen molecular ion with a few-pulse attosecond pulse train", Nat. Commun., 7, pp. 1-11, 2016.

[6] Heslar, J., Telnov, D.A., and Chu, S.I., "Enhancement of VUV and EUV generation by field-controlled resonance structures of diatomic molecules", Phys. Rev. A, 93(6), 2016.

[7] Chini, M., "Coherent phase-matched VUV generation by field-controlled bound states", Nat. Photonics, 8(6), pp. 437-441, 2014.

[8] Li, P.C., Jiao, Y.X., Zhou, X.X., and Chu, S.I., "Role of quantum trajectory in high-order harmonic generation in the Keldysh multiphoton regime", Opt. Expr., 24(13), pp. 14352-14361, 2016.

[9] Li, P.C., Sheu, Y.L., Laughlin, C., and Chu, S.I., "Role of laser-driven electron-multirescattering in resonance-enhanced below-threshold harmonic generation in He atoms", Phys. Rev. A, 90(4), pp. 1-5, 2014

[10] Fox, M.: 'Optical properties of solids' (Oxford University Press, 2001).

[11] Ghimire, S., "Observation of high-order harmonic generation in a bulk crystal", Nat. Phys., 7(2), pp. 138-141, 2011.

[12] McDonald, C.R., Vampa, G., Orlando, G., Corkum, P.B., and Brabec, T., "Theory of high-harmonic generation in solids", J Phys Conf Ser, 594, 2015.

[13] Vampa, G., "Theoretical Analysis of High-Harmonic Generation in Solids", Phys. Rev. Lett., 113(7), pp. 5, 2014.

[14] https://physics.nist.gov/PhysRefData/ASD/ionEnergy.html, accessed 30 Jan 2018.

[15] Shen, Y.R.: 'The principles of nonlinear optics' (J. Wiley, 1984).

[16] Spielmann, C., "Generation of coherent X-rays in the water window using 5-femtosecond laser pulses", Science, 278(5338), pp. 661-664, 1997.

[17] Zuffi, A.V.F.: 'Geração de harmônicos perturbativos por pulsos laser ultracurtos em gases nobres'. Dissertação (Mestrado em Ciências), Universidade de São Paulo, 2018.

[18] Corkum, P.B., "Amplification of Picosecond 10-Mu-M Pulses in Multiatmosphere CO_2-Lasers", IEEE J. Quantum Elec., 21(3), pp. 216-232, 1985.

[19] Yablonovitch, E., "Spectral Broadening in Light Transmitted through a Rapidly Growing Plasma", Phys. Rev. Lett., 31(14), pp. 877-879, 1973.

[20] Popmintchev, T., "Phase matching of high harmonic generation in the soft and hard X-ray regions of the spectrum", P. Natl. Acad. Sci. USA, 106(26), pp. 10516-10521, 2009.

[21] Verdeyen, J.T., and Gerardo, J.B., "Application of Laser to Plasma Refractive Index Determination", Ann. NY Acad. Sci., 122(A2), pp. 676-684, 1965.

[22] Keldysh, L.V., "Ionization in Field of a Strong Electromagnetic Wave", Sov. Phys. JETP-USSR, 20(5), pp. 1307-1314, 1965.

[23] Mcpherson, A., "Studies of Multiphoton Production of Vacuum Ultraviolet-Radiation in the Rare-Gases", J. Opt. Soc. Am. B, 4(4), pp. 595-601, 1987.

[24] Popmintchev, T., "Bright Coherent Ultrahigh Harmonics in the keV X-ray Regime from Mid-Infrared Femtosecond Lasers", Science, 336(6086), pp. 1287-1291, 2012.